Mode-expansion theory for inhomogeneous meta-surfaces

Shiyi Xiao, Qiong He, Che Qu, Xin Li, Shulin Sun, and Lei Zhou*

(submitted to PRB)

State Key Laboratory of Surface Physics and Key Laboratory of Micro and Nano Photonic Structures (Ministry of Education), Fudan University, Shanghai, 200433, China

I. Motivations:

In previous works of gradient meta-surface, theoretical understandings were either based on heuristic Fermat-Huygens wave interference arguments or based on full-wave numerical simulations[1,2,3].

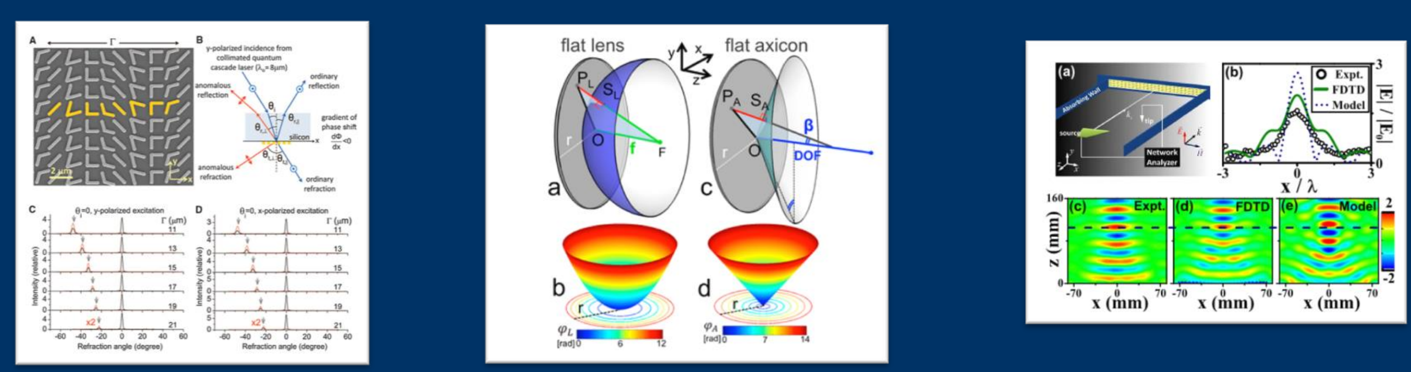

Fig. 1 Gradient meta-surface

PROBLEMS !

Is Fermat-Huygens enough?

Lack a theory framework

II. Developments of the mode-expansion theory

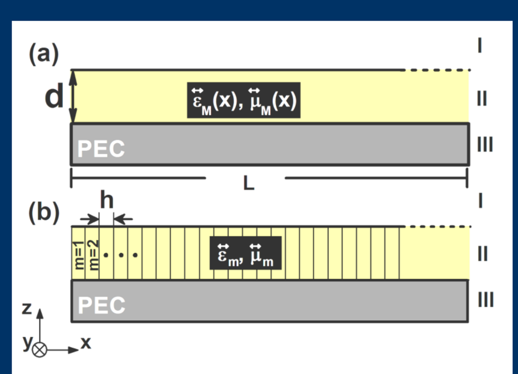

FIG. 2 (a) Geometry of the system under study. (b) Discretized model for the inhomogeneous structure.

The inhomogeneous MTM with permittivity and permeability matrices given by

$$\ddot{\varepsilon}_M(x)=\begin{pmatrix}\varepsilon_M^x(x) & 0 & 0\\ 0 & \varepsilon_M^y(x) & 0\\ 0 & 0 & \varepsilon_M^z\end{pmatrix},\ \ddot{\mu}_M(x)=\begin{pmatrix}\mu_M^x(x) & 0 & 0\\ 0 & \mu_M^y(x) & 0\\ 0 & 0 & \mu_M^z\end{pmatrix}.$$

Incident and reflected wave:

$$\begin{cases}\vec{E}^{in}(\vec{r})=e^{i(k_x^{in}x-k_z^{in}z)}\begin{pmatrix}0\\1\\0\end{pmatrix}\\ \vec{H}^{in}(\vec{r})=-\frac{1}{Z_0}e^{i(k_x^{in}x-k_z^{in}z)}\begin{pmatrix}k_z^{in}/k_0\\0\\k_x^{in}/k_0\end{pmatrix}\end{cases}\qquad \begin{cases}\vec{E}^{ref,n}(\vec{r})=e^{i(k_x^{r,n}x+k_z^{r,n}z)}\begin{pmatrix}0\\1\\0\end{pmatrix}\\ \vec{H}^{ref,n}(\vec{r})=\frac{1}{Z_0}e^{i(k_x^{r,n}x+k_z^{r,n}z)}\begin{pmatrix}k_z^{r,n}/k_0\\0\\-k_x^{r,n}/k_0\end{pmatrix}\end{cases}$$

Here, $k_0=\omega/c$ is the wave vector in vacuum with ω being the working frequency and c the speed of light.

The eigenmode in meta-surface region is:

$$E_y^{\pm}(q_z,x,z)=G(q_z,x)e^{\mp iq_z z}$$

where superscript, + and - stands for forward (+) and backward (-) propagating waves.

Here, G-function should be the result of

$$\frac{\mu_M^x(x)}{\mu_M^z}\frac{d^2G(q_z,x)}{dx^2}+\left[k_0^2\varepsilon_M^y(x)\mu_M^x(x)-q_z^2\right]G(q_z,x)=0$$

Matching boundary condition

$$\begin{cases}e^{ik_x^{in}x_m}+\sum_n\rho(k_x^{r,n})e^{ik_x^{r,n}x_m}=\sum_j G(q_{z,j},m)\left[C^+(q_{z,j})+C^-(q_{z,j})\right]\\ \frac{k_z^{in}}{k_0}e^{ik_x^{in}x_m}-\sum_n\rho(k_x^{r,n})\frac{k_z^{r,n}}{k_0}e^{ik_x^{r,n}x_m}=\sum_j\frac{q_{z,j}}{\mu_m^x k_0}G(q_{z,j},m)\left[C^+(q_{z,j})-C^-(q_{z,j})\right]\end{cases}$$

Reflection coefficients:

$$\rho(k_x^{r,n})=\sum_j A^{-1}(k_x^{in},q_{z,j})B(q_{z,j},k_x^{r,n})$$

where we have introduced two matrixes defined as:

$$\begin{cases}A(q_{z,j},k_x^{in})=\frac{k_z^{r,n}}{k_z^{r,n}+k_z^{in}}S(q_{z,j},k_x^{r,n})+\frac{k_z^{in}}{k_z^{r,n}+k_z^{in}}S'(q_{z,j},k_x^{r,n})\\ B(q_{z,j},k_x^{r,n})=\frac{k_z^{in}}{k_z^{r,n}+k_z^{in}}S(q_{z,j},k_x^{n})-\frac{k_z^{in}}{k_z^{r,n}+k_z^{in}}S'(q_{z,j},k_x^{r,n})\end{cases}$$

with

$$\begin{cases}S(q_{z,j},k_x^{r,n})=\frac{1}{L}\sum_m h(1-e^{i2q_{z,j}d})G(q_{z,j},m)e^{-ik_x^{r,n}mh}\\ S'(q_{z,j},k_x^{r,n})=-\frac{1}{L}\sum_m h\frac{q_{z,j}}{\mu_m^x k_z^{in}}(1+e^{i2q_{z,j}d})G(q_{z,j},m)e^{-ik_x^{r,n}mh}\end{cases}$$

III. Applications of the theory

Linearly varying reflection-phase profile:

$$\Phi(x)=\Phi_0+\xi x$$

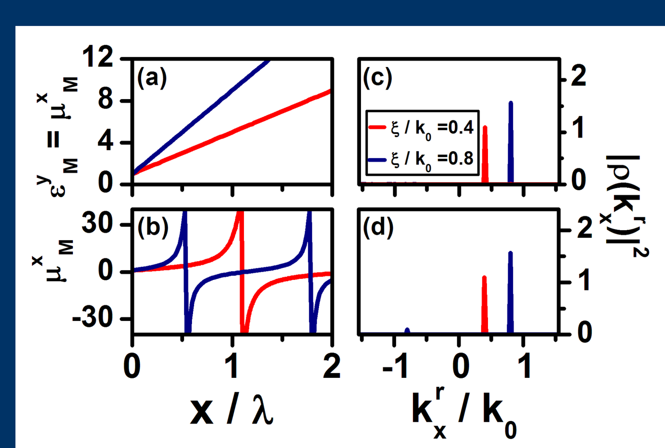

Fig.3 (a) Material properties. (b) Calculated scattering coefficients.

The generalized Snell's law:

$$k_x^r=\xi+k_x^{in}$$

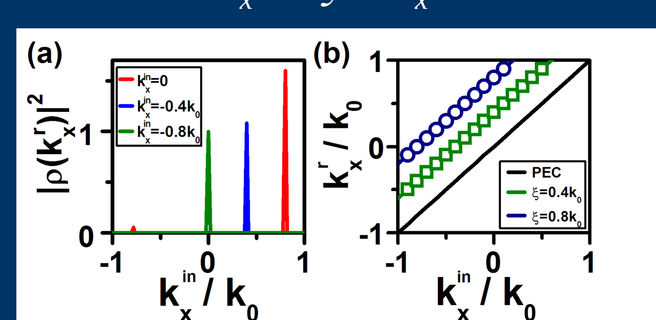

Fig.4 (a) Calculated scattering coefficients (b) angler dependency.

Parabolic reflection-phase distribution:

$$\Phi(x)=\Phi_0-k_0\sqrt{x^2+l_{focus}^2}+k_0\cdot l_{focus}$$

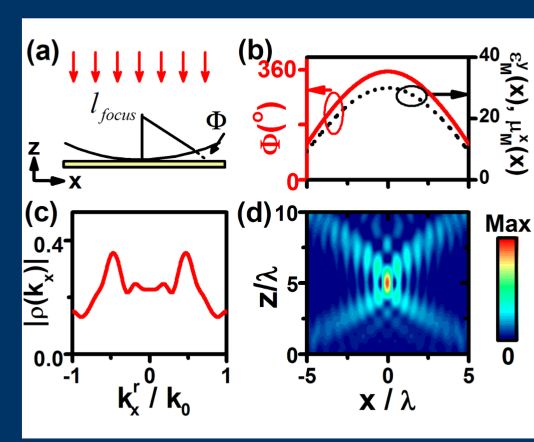

Fig.5 (a) Working scheme of the flat meta-surface lens, (b) Distributions of the parameter values and the reflection-phase. (c) Calculated spectrum. (d) Calculated E-field distribution .

IV. Comparisons with the local response model

With local approximation and neglecting near-field correction.

$$\rho_{\rm LRM}(k_x^r)=-e^{2ik_0 d}\delta(k_x^r-k_x^{in}-\xi)$$

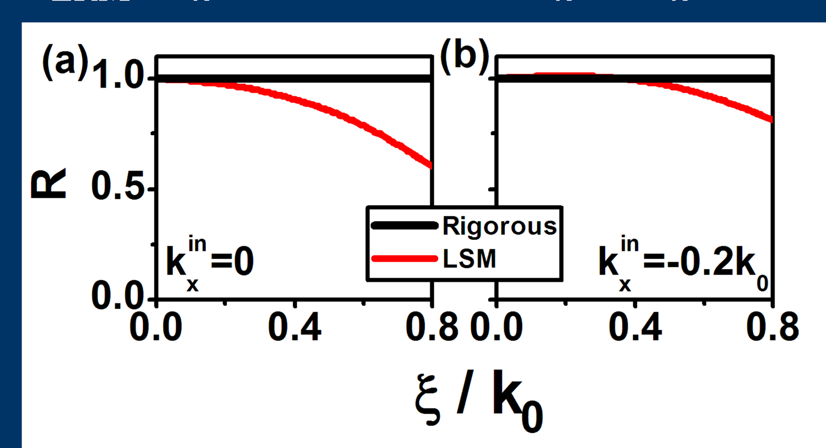

FIG. 6. (color online) Calculated reflectance of rigorous mode expansion method (black line) and local model (red line) versus ξ/k_0

V. Experimental and simulation verifications

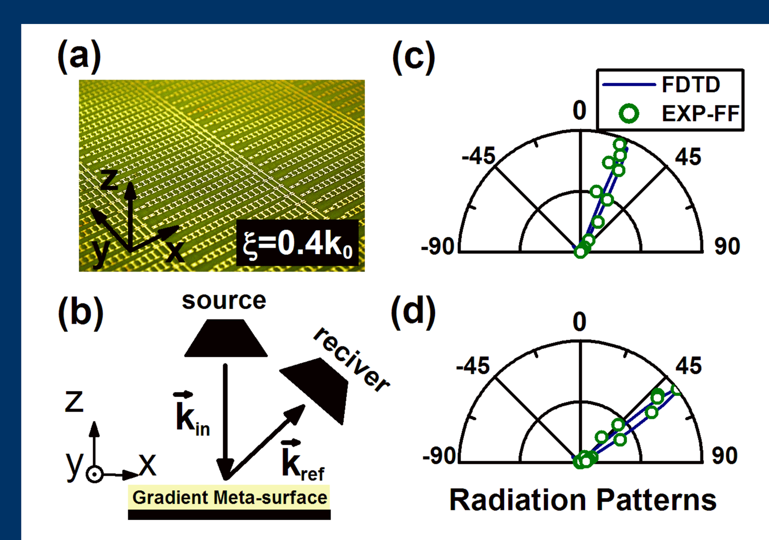

Fig.7. (a) Picture of part of the fabricated sample. (b) Schematics of the far-field characterization. (c) and (d) Measured (scatters) and simulated (lines) scattering patterns.

Conclusions:

1) Established a general theoretical framework.
2) Applied it to two particular examples as applications.
3) Full theory could go back to local response model under several simplifications.
4) local response model has energy non-conservation problems.
5) Microwave experiments match theoretical predictions .

[1] Science 334, 333 (2011)
[2] Nano Lett. 12, 1702 (2012)
[3] Opt. Lett. 37, 4940 (2012)